RESEARCH PAPER

Multi-Target Molecular Docking and Dynamics of Glycyrrhiza glabra Phytochemicals Against AChE and BChE in Alzheimer's Disease

Ishrat Jahan[1,2], Mohd Zakir[1,2], Saima Khan[1,2], Mohd Khubaib[1,2*]

[1]Molecular Immunology Laboratory, Integral Centre of Excellence for Interdisciplinary Research, Integral University, Lucknow (226026), Uttar Pradesh, India

[2]Department of Biosciences, Faculty of Science, Integral University, Kursi Road, Lucknow (226026), Uttar Pradesh, India

Corresponding Author: Dr. Mohd Khubaib, Assistant Professor, Department of Biosciences, Integral University, Lucknow

Email: khubaib.bio@gmail.com

Received: 15th Jul, 2026 | Revised: 25th Jul, 2026 | Accepted: 5th Aug, 2026 | Available Online: 12th Aug, 2026

Abstract

Abnormality in cholinergic neurotransmission is an important reason for the occurrence of cognitive deficits associated with Alzheimer's disease (AD). The two major enzymes responsible for the degradation of acetylcholine, namely acetylcholinesterase (AChE) and butyrylcholinesterase (BChE), represent key targets in the quest to develop cholinergic function-enhancing drugs. The demand for structurally diverse and potentially less toxic lead molecules arises from challenges with the efficacy, selectivity, and adverse effects of existing cholinesterase inhibitors. *Glycyrrhiza glabra* L. *is* a pharmacologically rich medicinal plant and represents a potential natural source of cholinesterase inhibitors. In this study, Pinocembrin and Liquiritigenin were selected as inhibitors of AChE and BChE. Based on docking scores and interaction mechanisms, Pinocembrin and Liquiritigenin emerged as the most suitable dual-targeting compounds among the 40 metabolites that showed good docking interactions with the target enzymes. Through complementary hydrogen bonding, hydrophobic interactions, π-π stacking, and other non-covalent interactions, both compounds exhibited sustained interactions at the catalytic/active sites of the target enzymes. The integrity and favourable interaction profiles of the selected complexes were maintained throughout the entire simulation duration through the study of backbone root-mean-square deviation, radius of gyration, solvent-accessible surface area, ligand activity, and hydrogen bonding. Overall, the findings suggest that Pinocembrin and Liquiritigenin are potential flavonoid frameworks from *G. glabra* that exhibit a dual inhibition profile for AChE and BChE. This integrative computational strategy provides a rational basis for selecting candidate drugs against AD-associated conditions.

Keywords: Alzheimer's disease, *Glycyrrhiza glabra*, Acetylcholinesterase, Butyrylcholinesterase, Pharmacological.

How to cite this article: Jahan I, Zakir M, Khan S, Khubaib M., Multi-Target Molecular Docking and Dynamics of Glycyrrhiza glabra Phytochemicals Against AChE and BChE in Alzheimer's Disease. Int J Drug Deliv Technol. 2026;16(78s): 1265-1280; DOI: 10.25258/ijddt.16.78s.175

1. Introduction

One of the major reasons of dementia around the world is Alzheimer's disease

(AD), which is a progressive disease of the nervous system (Breijyeh and Karaman, 2020). It consists of a complicated combination of processes rather than a simple molecular malfunction and is manifested through deterioration of memory, cognition, and nerve functioning (Payen et al., 2025). Since acetylcholine is responsible for learning, memory, attention, and cognitive functions, malfunctioning of cholinergic transmission has been receiving quite much attention as one of the principal changes associated with AD (Ballinger et al., 2016). While butyrylcholinesterase (BChE) plays a role in cholinergic regulation and becomes more important as the disease develops, acetylcholinesterase (AChE) is an enzyme primarily responsible for the fast breakdown of acetylcholine (Ballinger et al., 2016). Consequently, the simultaneous control of AChE and BChE activities has gained a lot of consideration as a suitable strategy for maintaining cholinergic neurotransmission in AD. In addition to the conventional role in acetylcholine metabolism, BChE has attracted considerable attention recently, making it worth considering as one of the principal therapeutic targets for AD treatment (Xing et al., 2021). While they relieve the symptoms, currently existing cholinesterase inhibitors, including those used in therapy, do not inhibit the pathological process itself. The development of structurally diverse ligands that will bind to cholinesterase targets has been promoted by certain restrictions related to tolerance, target selectivity, and efficacy of therapies. *G. glabra* plants contain structurally diverse metabolites with various pharmacological properties and chemical frameworks; natural compounds provide a highly attractive chemical space. Licorice (*G. glabra L.,* Fabaceae) is a medicinal plant with a diverse chemical profile involving flavonoids, flavanones, chalcones, coumarins, triterpenoids, and their associated secondary metabolites (Xing et al., 2021). *G. glabra* is an interesting medicinal plant source of multifunctional compounds in relation to neurodegenerative disorders, since some of its components have been reported to have antioxidant, anti-inflammatory, antibacterial, and neuropharmacological activities. Pinocembrin and Liquiritigenin are among the flavonoids of *G. glabra* that are especially interesting due to their beneficial structural features and biological activity (Cerulli et al., 2022). Liquiritigenin and its analogues have previously been studied for their cholinesterase inhibitory activity and as anti-Alzheimer's compounds (Nour et al., 2023). In particular, liquiritigenin derivatives have demonstrated an interaction with cholinesterase targets, and computational studies have been conducted to investigate their binding and dynamics towards BChE (Arora et al., 2025). Nevertheless, a sufficient number of studies have not been carried out in terms of a comprehensive investigation of *G. glabra* secondary metabolites in relation to both AChE and BChE, after which comparative selection and long-time-scale MD simulation will be performed. Thus, for the purpose of investigating the potential of *G. glabra* secondary metabolites as dual cholinesterase targets, the current research was developed. Molecular docking studies using AChE and BChE on secondary metabolites from *G. glabra* were conducted (El-Nashar et al., 2025). After a comparative analysis of the favourable interactions between the potential compounds and the two targets,

Pinocembrin and Liquiritigenin were selected. After the selection of the protein-ligand complexes, the complexes were further subjected to 100-ns molecular dynamics simulation studies to analyse conformational stability, flexibility, compactness, solvent exposure, hydrogen bond stability, and concerted motion. For a better understanding of the energetic role of protein-ligand interactions, binding free-energy calculations were carried out when necessary. This work aimed to develop a structure-based computational approach to identify potential AChE/BChE targeting ligands from G. glabra (Bhatt et al., 2022). Computer-aided drug design (CADD) is an emerging computational method in modern drug discovery, providing an efficient way to systematically screen, evaluate, and optimise prospective drugs using structure- and ligand-based computations (Macalino et al., 2015). The major aspects of CADD include molecular modelling, virtual screening, molecular docking, pharmacokinetic and toxicity predictions, and molecular dynamics simulations, which study the interactions between bioactive molecules and disease-related molecular targets (Yuan et al., 2025). Computational methods can save time, money, and the number of molecules needed for drug discovery compared to traditional screening methods by selecting prospective molecules for further experimental validation (Fahim, 2026). Molecular docking helps understand the binding mode and affinity of the ligands, while molecular dynamics simulations provide the dynamics study of the protein-ligand complex under physiological conditions . Moreover, *in silico* ADMET and drug-likeness predictions will be able to evaluate the pharmacokinetic characteristics and toxicity of the molecules at an early stage. Therefore, the combination of CADD methods allows one to apply a rational and efficient approach to the screening of natural products and selection of lead molecules for therapy development (Llorach-Pares et al., 2022).

2. Materials and Methodology

2.1 Protein structure preparation

The 3D structures of human AChE (PDB ID: 1U65) and BChE (PDB ID: 4PM8) proteins were obtained from the RCSB Protein Data Bank (PDB) https://www.rcsb.org/. The protein structures were preprocessed for docking by removing unwanted heteroatoms and crystallographic water molecules, adding hydrogen atoms, and assigning correct atomic charges. The missing atoms and residues were processed using Discovery Studio. After preprocessing, the protein structures were converted into docking format.

2.2 Ligand preparation

Ligand preparation was performed before docking of metabolites from *G. glabra.* Discovery Studio determined atomic charges and protonation. Structures of compounds were acquired from PubChem https://pubchem.ncbi.nlm.nih.gov/. To achieve energetically optimal conformations of ligands, energy minimisation was performed using the CHARMM force field.

2.3 ADMET Profiling

The ADMET and drug-likeness profiles of *G. glabra* secondary metabolites were evaluated using the web-based platforms SwissADME https://www.swissadme.ch/and ProTox-3.0 https://tox.charite.de/protox3/. Canonical SMILES of the compounds were used as input. SwissADME was employed to assess

physicochemical properties, including molecular weight (MW), iLOGP, topological polar surface area (TPSA), hydrogen-bond donors (HBD), hydrogen-bond acceptors (HBA), rotatable bonds, along with Lipinski's Rule of Five, gastrointestinal absorption, and blood–brain barrier (BBB) permeability. ProTox-II was used to predict toxicity class, hepatotoxicity, carcinogenicity, mutagenicity, cytotoxicity, and immunotoxicity. The obtained ADMET and toxicity profiles were used for preliminary screening and selection of compounds for subsequent molecular docking studies against AChE and BChE.

2.4 Molecular docking

In order to analyse the binding potential of the generated *G. glabra* metabolites against AChE and BChE, structure-based molecular docking analysis was performed. AutoDock4.2 version was used for the docking study. Grid generation was done for each target based on the experimentally determined active site of the enzyme. The docking score predicted for docking was used to rank the various poses obtained for each ligand. Using the docking score, pose ranking and binding site location, the best pose was selected. The docking score of the selected compounds for both targets was compared.

2.5 Molecular Dynamics Simulation and Trajectory Analysis

For MD simulation, the best docking complex was used to analyse the complex stability over a 100 ns timeframe. SwissParam software creates ligand structure and coordinate files that can be recognised by the CHARMM36 all-atom force field while doing MD simulations. In a similar vein, the protein's topology and coordinate files were created using the pdb2gmx function of GROMACS 2023.2, which was compatible with the CHARMM36 force field. Under periodic boundary conditions, each protein-ligand combination was placed in the centre of a triclinic box that was filled with TIP3P water molecules and was kept at least 1 nm from the box wall. To relax the systems, energy minimisation was applied for a maximum of 50,000 steps. The steepest descent approach was used to perform energy minimisation steps, using a convergence criterion of 100.0 kJ mol−1 nm−1. The system was then subjected to two stages of equilibration, each lasting 1000 ps, to bring it to 310 K and 1 bar, replicating physiological circumstances. A constant number of particles, temperature, and volume were used for the first equilibration, whereas a constant number of particles, temperature, and pressure were used for the second equilibration. The velocity-rescale thermostat and the Parrinello-Rahman pressure coupling approach were used to maintain temperature and pressure stability. The MD simulation production process was then completed with a simulation time of 100 ns, performed at 310 K and 1 bar with an integration time of 2 fs at physiological conditions. The results of the MD simulations were examined using plots of RMSD, root mean square deviation fluctuation (RMSF), the radius of gyration (Rg), solvent accessible surface area (SASA), and H-bonds. The following Gromacs modules were used to analyse the MD trajectories: gmx rms, gmx rmsf, gmx gyrate, make_ndx, gmx hbond, gmx anaeig, gmx sham, gmx_covar, and gmx sasa for the calculation of RMSD, RMSF, Rg, SASA, and H-bond plots. Xmgrace 5.1.25 was used to create the graphs and figures.

3. Results

3.1 ADMET Profiling

Based on their physicochemical, drug-like, pharmacokinetic, and toxicity parameters, both pinocembrin and liquiritigenin possessed promising characteristics for further exploration as possible anti-Alzheimer's drug leads. Both molecules had identical molecular weight (256.25 Da), molecular formula ($C_{15}H_{12}O_4$), rotatable bonds (1), and TPSA (66.76 Å²). Differences in LogP and hydrogen-bonding characteristics could be noted. Pinocembrin had a LogP value of 2.11 with 2 hydrogen-bond donors and 4 acceptors, while liquiritigenin had a lower LogP (1.73) and 4 hydrogen-bond donors. Both molecules conformed to Lipinski's rule of five without violations and were considered to have high gastrointestinal permeability and good blood-brain barrier permeability, which is highly desirable for drugs targeting Alzheimer's disease. Neither molecule was a substrate for P-glycoprotein. Both compounds were shown to have predicted inhibition of CYP1A2 and CYP2C19, while pinocembrin was not shown to inhibit CYP2C9 and CYP3A4, but liquiritigenin inhibited both enzymes. Notably, both compounds were shown to lack mutagenicity, hepatotoxicity, neurotoxicity, and immunotoxicity. Thus, these ADMET studies suggested promising preliminary safety of these molecules, as shown in Table 1. The obtained results supported the selection of both pinocembrin and liquiritigenin for further molecular docking and molecular dynamics studies towards AChE and BChE.

Table 1: Physicochemical, Lipinski and ADMET profiles of Pinocembrin and Liquiritigenin

Parameter	**Pinocembrin**	**Liquiritigenin**
Molecular weight (Da)	256.25	256.25
Molecular formula	C15H12O4	C15H12O4
LogP	2.11	1.73
H-bond donors	2	4
H-bond acceptors	4	1
Rotatable bonds	1	1
TPSA (Å²)	66.76	66.76
Lipinski violations	0	0
GI absorption	High	High
BBB permeability	Yes	Yes
P-gp substrate	No	No
CYP1A2 inhibition	Yes	Yes
CYP2C19 inhibition	Yes	Yes
CYP2C9 inhibition	No	Yes
CYP2D6 inhibition	No	No
CYP3A4 inhibition	No	Yes
Mutagenicity	Inactive	Inactive
Hepatotoxicity	Inactive	Inactive
Neurotoxicity	Inactive	Inactive
Immunotoxicity	Inactive	Inactive

3.2 Molecular Docking Analysis

Blind molecular docking was performed using a set of 40 selected secondary

metabolites of *G. glabra* against (AChE) and (BChE) in order to discover metabolites with favorable binding properties against both cholinesterases. The docking study offered a comparative evaluation of the binding energies and interaction behaviors of the selected metabolites. The full details of the blind-docking results, comprising the binding energy predictions for all 40 compounds against AChE and BChE, are presented in Supplementary Table S1.

Among the metabolites exhibiting good binding towards both targets, further analysis with regard to the drug-likeness and toxicity features was done in order to choose promising compounds that have the right physical and chemical features and low toxicity. As a result of such an integrated screening, pinocembrin and liquiritigenin were chosen as the most prospective candidates for further structural analysis and molecular dynamic simulation studies. The comparative docking scores and interaction behaviors of pinocembrin and liquiritigenin with AChE and BChE are shown in Table 2.

Figure 1 represents the 2D and 3D interaction profiles of pinocembrin and liquiritigenin at the active sites of BChE and AChE. The presence of multiple non-covalent interactions between these compounds and the residues surrounding the active site cavity suggested good recognition of the ligands by the proteins. Liquiritigenin was present in the aromatic-rich gorge of the AChE–liquiritigenin complex (Figure 1 a,b), interacting with a variety of important residues, such as Trp84, Tyr121, Ser122, Gly117, Gly118, Glu199, Tyr130, Phe330, Phe331, Tyr334, and Ile444. The interaction profile comprised mainly van der Waals and covalent interactions, which helped to maintain the ligand inside the AChE gorge. In addition, the aromatic rings like Phe330, Phe331, and Tyr334 surrounded the aromatic ring system of liquiritigenin, which provided good π-interactions between the ligand and enzyme. In the case of the pinocembrin-AChE complex, a similar occupation was observed in the active site pocket (Figure 1 c,d). All residues like Tyr121, Ser122, Gly117, Gly118, Gly123, Trp84, Glu199, Tyr130, Phe330, Phe331, and Tyr334 were involved in interactions with pinocembrin. Interactions with Phe330 and Tyr334 further strengthened the aromatic moiety of pinocembrin, while several van der Waals interactions complemented the overall binding environment. Such interactions indicate that the same aromatic binding site on AChE can favourably bind pinocembrin. The BChE-liquiritigenin complex (Figure 1 e,f) bound with Trp82, Ala328, Val331, Tyr332, Trp430, Met437, Glu197, Tyr128, Gly115, Gly116, Gly121, and Thr120 within the active site cavity. Gly121 displayed a typical hydrogen bond interaction, while Trp82 established a π-stacking interaction. The aromatic ring of liquiritigenin established hydrophobic/π-stacking interactions with Ala328 and adjacent aromatic residues, like Tyr332 and Trp430. The same kind of interactions between Glu197, Tyr128, Gly115, Gly116, Gly121, Thr120, Gly439, Trp430, Met437, Tyr332, Trp82, and Ala328 were seen in BChE–pinocembrin (Figure 1 g,h). There was an interaction of carbon-hydrogen interaction involving Gly439, along with typical hydrogen bonding with Glu197. In addition to that, there was a contribution of a π-alkyl interaction from Ala328, and there was also a π-π interaction. For liquiritigenin and pinocembrin, in the AChE and BChE enzyme pockets, various complementary

interactions were observed, including hydrogen bonding, π-π/π-stacking, hydrophobic interactions, and van der Waals forces. Their good fitting into the two cholinesterase pockets is attributed to their interactions with many aromatic and gorge residue components, including Trp84/Phe330/Tyr334 for AChE and Trp82/Ala328/Tyr332/Trp430 for BChE. Liquiritigenin and pinocembrin could be regarded as potential lead compounds against cholinesterases that can be further validated by molecular dynamics simulations and experiments.

Target	Compound	Binding energy (Kcal/ mol)	Active site residues	H-bonds interacting with the amino acid
AChE	Liquiritigenin	-9.9	TRP84, TYR121, SER122, GLY117, GLY118, GLU199, TYR130, PHE330, PHE331, TYR334, and ILE444	GLU199, TYR130, PHE330
	Pinocembrin	-10.7	TYR121, SER122, GLY117, GLY118, GLY123, TRP84, GLU199, TYR130, PHE330, PHE331, and TYR334	TYR130
BChE	Liquiritigenin	-9.0	TRP82, ALA328, VAL331, TYR332, TRP430, MET437, GLU197, TYR128, GLY115, GLY116, GLY121, and THR120	GLY121
	Pinocembrin	-9.2	GLU197, TYR128, GLY115, GLY116, GLY121, THR120, GLY439, TRP430, MET437, TYR332, TRP82, and ALA328	GLU197

Table 2: Molecular docking Binding energy of Glabridin compounds with (GSK3β), (MAO-B), and (BACE1)

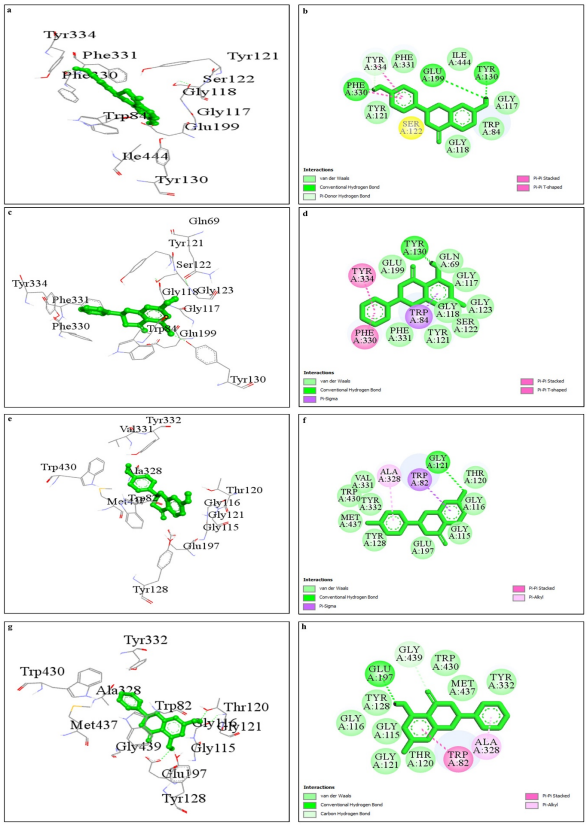

Figure 1: 3D & 2D structural representation of (a,b) AChE-Liquiritigenin (c,d) AChE-Pinocembrin (e,f) BChE-Liquiritigenin (g,h) BChE-Pinocembrin

3.3 Molecular Dynamics Simulation Analysis

Table 3 provides a detailed overview of how three ligands—glabridin, liquiritigenin, and pinocembrin—interact with two enzymes, ACHE (Acetylcholinesterase) and BUCHE (Butyrylcholinesterase), based on MD (molecular dynamics) simulation results. Here's a breakdown of each property and what it reveals about the interaction dynamics and structural behaviour of these ligands with the enzymes.

Table 3: MD simulation of Liquiritigenin & Pinocembrin with the two major Alzheimer's disease target proteins, Acetylcholinesterase and butyrylcholinesterase

MD simulation property	AChE		BChE	
	Liquiritigenin	Pinocembrin	Liquiritigenin	Pinocembrin
RMSD protein Backbone (nm)	0.000498633-0.249933	0.0004952-0.2176445	0.000504-4.422238	0.0005046-4.68428
RMSD lig-fit on protein (nm)	0.0005122-0.4006881	0.0005032-0.3368063	0.0005354-9.4763145	0.0005299-11.519
RMSF protein Backbone (nm)	0.0318-0.8194	0.0337-0.8572	0.7416-3.4588	0.7841-3.1579
Ligand Radius of gyration (nm)	0.348063-0.369528	0.331535-0.349216	0.348394-0.369432	0.33261-0.34955
Ligand Solvent Accessible Surface (nm^2)	3.961-5.36	3.909-5.288	3.898-5.305	3.932-5.293

Coul-SR: Protein LIG (kJ/mol)	-122.53 ±23.29	-64.6787 ±29.706	-70.861 ±23.28	-39.468 ±25.142
LJ-SR:Protein-LIG (kJ/mol)	-120.979 ±10.59	-116.549 -9.40	-110.59 ±9.926	-111.557 ±11.513

3.3.1 AChE–Liquiritigenin Complex

Stability analysis of the AChE-ligand complex was done using a 100 ns molecular dynamics simulation with ligand-fit RMSD, protein backbone RMSF, radius of gyration, solvent-accessible surface area (SASA), hydrogen bonding formation and interaction energy data shown in Figure 2. Ligand fit RMSD analysis shows that the RMSD for liquiritigenin was maintained within the 0.0005122- 0.4006881 nm range, which indicates that there were limited positional variations of the ligand within the binding pocket of AChE. From the above findings, it is reasonable to assume that the binding of liquiritigenin with AChE was relatively stable since there were minimal changes in the RMSD of the ligand. The analysis of protein backbone RMSF revealed that there was moderate flexibility of the amino acid residues, which means that the binding of liquiritigenin with AChE did not destabilise the structure of ACHE. The restriction in the backbone flexibility further supports the stability of the enzyme-ligand complex. The radius of gyration of liquiritigenin was maintained in a relatively compact range, where the maximum value was approximately 0.37 nm. This indicates that the ligand maintained a stable molecular conformation throughout the simulation period.

SASA profile analysis shows that liquiritigenin had limited solvent exposure compared to the exposed ligand configuration. The above finding indicates that a significant portion of the ligand remained accommodated in the hydrophobic and partly buried AChE binding pocket. Analysis of hydrogen bond interactions revealed that the hydrogen bond interaction persisted between liquiritigenin and AChE throughout the simulation process, and at least 2-3 hydrogen bonds were maintained. From the above hydrogen bonding, it can be assumed that hydrogen bonds played an important role in the stability of the complex. Short-range interaction energy analysis further supports the favourable association of liquiritigenin with AChE. The short-range Coulombic interaction energy (Coul-SR) was approximately -122.53 kJ/mol, which means that there were favourable electrostatic interactions between the ligand and the protein. In addition, the short-range Lennard-Jones interaction energy (LJ-SR) was approximately -120.979 kJ/mol, which indicates favourable van der Waals interactions within the binding pocket.

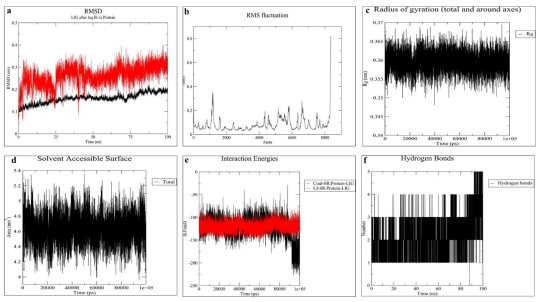

Figure 2: Molecular Dynamics Simulation of AChE- Liquiritigenin Complex: (a) RMSD (b) RMSF (c) Radius of Gyration

(d) Solvent Accessible Surface (e) Interaction Energy (f) Hydrogen Bond

3.3.2 AChE–Pinocembrin Complex

The dynamic properties of the AChE-pinocembrin complex were analysed with the same trajectory-based parameters. Pinocembrin revealed ligand-fit RMSD values that ranged from 0.0005032 to 0.3368063 nm, which is indicative of rather small fluctuations in the position of the ligand throughout the 100 ns simulation. Low RMSD values mean that pinocembrin retained its position in the binding cavity without displacing from the initial binding site. The backbone RMSF values show rather moderate fluctuations of the residues, meaning that the formation of the AChE-pinocembrin complex did not cause any structural changes in the receptor. The stability of the protein backbone structure means that the complex maintained its structure throughout the simulation. The radius of gyration of the ligand was also rather low, with a maximum value of approximately 0.37 nm, which means that pinocembrin maintained its compact conformation during the simulation. SASA analysis also indicates low solvent accessibility of pinocembrin, which means that the ligand was accommodated in the binding cavity. Rather stable SASA values suggest that pinocembrin maintained its interaction environment throughout the simulation. The hydrogen bond analysis showed that pinocembrin formed a maximum of three hydrogen bonds with AChE, with 1-2 hydrogen bonds being preserved for most of the simulation time. Despite the fact that fewer hydrogen bonds persisted throughout the simulation compared with liquiritigenin, their preservation means that hydrogen bonding played an important role in stabilising the ligand inside the binding pocket. The interaction energy analysis showed favourable non-bonded interactions between pinocembrin and ACHE. The Coul-SR interaction energy was approximately −64.6787 kJ/mol, which indicates the presence of favourable electrostatic interactions. The LJ-SR interaction energy was approximately −116.549 kJ/mol, which indicates the presence of favourable van der Waals interactions. Overall, the low ligand RMSD, moderate protein backbone fluctuations, ligand conformation, solvent accessibility, hydrogen bonds, and interaction energies suggest that the interaction of pinocembrin with the AChE binding pocket remained stable during the 100 ns simulation in Figure 3.

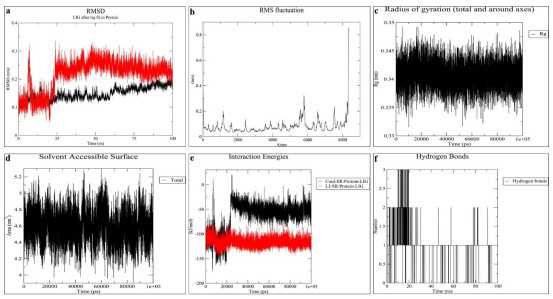

Figure 3: Molecular Dynamics Simulation of AChE- Pinocembrin Complex: (a) RMSD (b) RMSF (c) Radius of Gyration (d) Solvent Accessible Surface (e) Interaction Energy (f) Hydrogen Bond

3.3.3 BChE–Liquiritigenin Complex

In addition, the stability of the BChE-liquiritigenin complex was assessed by analysing the ligand RMSD, protein backbone RMSF, radius of gyration, SASA, and hydrogen-bonding and non-bonded interaction energies, as shown in Figure 4. Unlike the ACHE-liquiritigenin complex, liquiritigenin showed larger positional fluctuations in the case of interaction with BChE, which means higher ligand mobility inside the binding site. BChE backbone RMSF demonstrated higher residue

fluctuations, which is reflected in the fact that RMSF reached approximately 3.4588 nm during the course of the simulation. High RMSF means increased local flexibility of the protein and suggests that the BChE structure underwent larger conformational changes during ligand binding. The radius of gyration of liquiritigenin was relatively compact during the simulation, being approximately equal to 0.37 nm. Thus, although the position of liquiritigenin in the pocket changed, it kept its relatively compact conformation. The SASA profile of liquiritigenin remained largely unchanged compared to the ACHE complex. Thus, similar SASA and higher RMSD/RMSF suggest that the ligand underwent large movements inside the binding pocket but did not change its solvation significantly. Hydrogen bond analysis showed that liquiritigenin maintained 2-3 hydrogen bonds with BChE for most of the 100 ns simulation. Thus, hydrogen bonding between BChE and liquiritigenin persisted for a large part of the simulation. However, even hydrogen bonding does not guarantee full stability of the ligand in its binding site due to higher RMSD and RMSF. In general, the BChE-liquiritigenin complex demonstrated hydrogen bonding and a relatively compact ligand conformation, but higher fluctuations than the corresponding ACHE complex. These results suggest that although liquiritigenin interacted with BChE, it was more mobile inside the binding site.

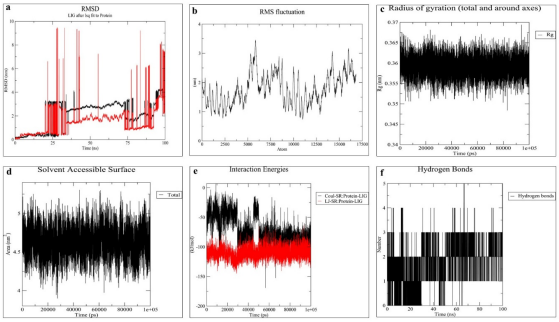

Figure 4: Molecular Dynamics Simulation of BChE-Liquiritigenin Complex: (a) RMSD (b) RMSF (c) Radius of Gyration (d) Solvent Accessible Surface (e) Interaction Energy (f) Hydrogen Bond

3.3.4 BChE–Pinocembrin Complex

The BChE-pinocembrin complex was assessed during a 100 ns MD simulation as well. Pinocembrin possessed larger ligand positional fluctuations compared with the ACHE complex, revealing increased movement inside the binding site of BChE. Such behaviour is evidence that the ligand experienced larger conformational or positional rearrangements during the simulation. The protein backbone RMSF profile revealed higher residue flexibility in BChE than in the AChE complex. The higher fluctuations imply that BChE experienced larger local conformational changes during interaction with pinocembrin. However, the radius of gyration of the ligand was rather low, reaching approximately 0.37 nm, which implies that the internal compactness of the ligand was preserved during the simulation. The SASA profile revealed solvent exposure comparable to that observed for the ligand in the ACHE complex. This implies that pinocembrin experienced a similar level of solvent accessibility despite the larger dynamics of the BChE complex. Therefore, the higher dynamics of the ligand was not accompanied by high solvent exposure. Hydrogen-bonding

analysis demonstrated that pinocembrin formed up to three hydrogen bonds with BChE, where 1-2 hydrogen bonds were formed for most of the time. The existence of such hydrogen bonds implies that certain polar interactions were responsible for the ligand retention in the binding site, although the complex possessed higher dynamic fluctuations. The interaction energy profile implied favourable non-bonded interactions between the ligand and BChE. In particular, the short-range Coulombic interaction energy was approximately −64.8 kJ/mol, implying a favourable electrostatic contribution. At the same time, the LJ-SR interaction energy varied from approximately −110.59 to −118.40 kJ/mol, which implies favourable van der Waals interactions. Overall, the BChE-pinocembrin complex experienced hydrogen bonding and favourable non-bonded interactions but had higher dynamic fluctuations than the corresponding AChE complex in Figure 5.

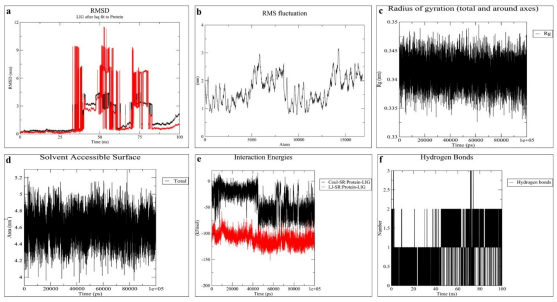

Figure 5: Molecular Dynamics Simulation of BChE-Pinocembrin Complex: (a) RMSD, (b) RMSF, (c) Radius of Gyration, (d) Solvent Accessible Surface, (e) Interaction Energy, (f) Hydrogen Bond

4.Discussion

To shed light on possible binding modes and interactions of pinocembrin and liquiritigenin with AChE and BChE, a molecular docking approach was performed (Cichon et al., 2024). As a result of docking studies, hydrogen-bonding, aromatic, hydrophobic, and van der Waals interactions between the ligands and residues of catalytic and peripheral pockets of the enzymes were identified, thus demonstrating favourable accommodation of the molecules inside the cholinesterase binding pockets (Figure 1) (Shah et al., 2026). Several complementary contacts suggest that the broad spectrum of interactions inside the enzyme pockets is involved in the binding of these molecules (Kufareva et al., 2012). The ligand in the AChE–liquiritigenin complex interacted with residues such as Trp84, Tyr121, Ser122, Gly117, Gly118, Glu199, Tyr130, Phe330, Phe331, Tyr334, and Ile444. In the AChE–liquiritigenin complex, the ligand made contact with residues such as Trp84, Tyr121, Ser122, Gly117, Gly118, Glu199, Tyr130, Phe330, Phe331, Tyr334, and Ile444. The ligand occupied the specific aromatic-rich gorge region of AChE. Since aromatic residues play a significant role in stabilising the flavonoid structure via hydrophobic and π-interactions, they are particularly important in the AChE gorge around the ligand (Ríos et al., 2026). The proper positioning of liquiritigenin in the AChE gorge is possibly due to interactions between Trp84, Phe330, Phe331, and Tyr334. Similarly, pinocembrin made contact with residues such as Tyr121, Ser122, Gly117, Gly118, Gly123, Trp84, Glu199, Tyr130, Phe330, and Phe331.

A similar tendency for significant accommodation of the ligand within the binding cavity of the enzyme was also observed for the BChE-ligand complexes. These residues such as Trp82, Ala328, Val331, Tyr332, Trp430, Met437, Glu197, Tyr128, Gly115, Gly116, Gly121, and Thr120 showed the reaction with liquiritigenin. In the case of the ligand, it can be held in a favourable orientation by

means of the hydrogen bond interaction between Gly121, π-associated interactions with Trp82, and contact with aromatic and hydrophobic residues. In addition to that, pinocembrin exhibited extensive interactions with Glu197, Tyr128, Gly115, Gly116, Gly121, Thr120, Gly439, and Trp82. Molecular docking is a relatively static structural modelling technique that does not fully take into account the dynamic nature of the protein-ligand complexes, even though the approach provides relevant information about the preferred binding orientation (Jin and Wei, 2024). To determine whether the suggested binding modes would be stable within the dynamic environment, 100-ns molecular dynamics (MD) simulations were performed for the AChE-liquiritigenin, AChE-pinocembrin, BChE-liquiritigenin, and BChE-pinocembrin complexes. The analysis of the protein backbone RMSD, the flexibility of protein residues using RMSF, radius of gyration, solvent-accessible surface area, ligand RMSD, and intermolecular hydrogen bonding during the simulation trajectory will give a more realistic insight into the stability of the complexes (da Fonseca et al., 2024). The overall stability of the protein conformations throughout the 100-ns simulation can be assessed through the backbone RMSD analysis of the four protein systems (Baammi et al., 2023). The four protein systems show a highly stable trajectory after the initial equilibration stage without any evidence of structural perturbation, which indicates that the structure of the cholinesterase was not affected much by the flavonoid binding (Mir et al., 2024). Due to the flexible nature of proteins and due to ligand-induced rearrangement, some variations in RMSD are expected in MD simulations. The stability of the docked complexes in dynamic conditions is indicated by the stable backbone trajectory of the simulation (Banavath et al., 2014). The dynamic stability of the AChE–liquiritigenin, AChE–pinocembrin, BChE–liquiritigenin, and BChE–pinocembrin complexes was confirmed by the 100-ns molecular dynamics simulations. Greater variations in the loop and termini regions indicated normal flexibility of the proteins, whereas RMSF analysis indicated restricted fluctuations in the proximity of the key residues of the binding sites (Tan et al., 2005). The compactness and integrity of the protein structure were maintained by stable profiles of Rg and SASA. Both flavonoids were still bound to their binding sites with minor conformational changes, as indicated by the stable ligand RMSD profiles. The stability of the docking-generated binding modes was confirmed by the recurring hydrogen-bonding between the key residues (Anil et al., 2026). It seems that liquiritigenin and pinocembrin generate stable interactions with both AChE and BChE, as evidenced by the docking and MD studies, thus proving their suitability as leads against cholinesterases and Alzheimer's disease (Nour et al., 2023). Inhibitory effects of the enzymes in experiments. Overall, the combined molecular docking and 100-ns MD simulation approach strengthens the structural interpretation of liquiritigenin and pinocembrin binding to AChE and BChE. The docking results reveal extensive interaction networks within the cholinesterase binding cavities, while the MD simulations provide a dynamic assessment of complex stability. These findings collectively support further experimental evaluation of liquiritigenin and pinocembrin as potential cholinesterase-targeting constituents of

Glycyrrhiza glabra and provide a computational basis for subsequent mechanistic and pharmacological investigations.

5. Conclusion

Liquiritigenin and pinocembrin have favourable binding affinities with both AChE and BChE, according to the current computational study. Multiple hydrogen-bonding, π-associated, hydrophobic, and van der Waals contacts were found in the cholinesterase binding sites by molecular docking, and the structural stability of the resultant complexes was confirmed by 100-ns molecular dynamics simulations. Both compounds may function as possible dual cholinesterase-targeting natural-product leads for Alzheimer's disease, according to the combined docking and MD results. To confirm their inhibitory effectiveness and mode of action, more experimental AChE/BChE inhibition and enzyme kinetic studies are required.

Author Contribution

Ishrat Jahan: Writing- original draft, Software, Resources, Formal analysis, Data curation, Conceptualisation; **Mohd Zakir:** Methodology; **Saima Khan:** Visualisation; **Mohd Khubaib:** Writing – review & editing, Visualisation, Validation, Supervision, Formal analysis.

Competing Interest

The authors declare they have no known competing financial or personal interests.

Acknowledgement

The authors express their gratitude towards Integral University, Lucknow, for providing the necessary facilities and Manuscript Communication Number (IU/R&D/2026-MCN0004900)

Funding

No funding

Refrencess

Anil, A., Tripathi, D., Nayak, S.S., Krishna, R., Kumar, U., Manimaran, B., Sakthivel, N., 2026. Elucidation of the molecular binding mechanism of an anticancer thiolato-bridged manganese (I) carbonyl complex with apotransferrin: Thermodynamic and structural insights. Biochem. Biophys. Res. Commun. 154135. https://doi.org/10.1016/j.bbrc.2026.154135

Arora, P., Swati, Rani, S., Jha, S., Gupta, S., Kumar, S., 2025. Innovative approaches in acetylcholinesterase inhibition: a pathway to effective Alzheimer's disease treatment. Mol. Divers. 29, 5367–5396. https://doi.org/10.1007/s11030-025-11170-1

Baammi, S., Daoud, R., El Allali, A., 2023. *In silico* protein engineering shows that novel mutations affecting NAD+ binding sites may improve phosphite dehydrogenase stability and activity. Sci. Rep. 13, 1878. https://doi.org/10.1038/s41598-023-28246-3

Ballinger, E.C., Ananth, M., Talmage, D.A., Role, L.W., 2016. Basal forebrain cholinergic circuits and signalling in cognition and cognitive decline. Neuron 91, 1199–1218. http://dx.doi.org/10.1016/j.neuron.2016.09.006

Banavath, H.N., Sharma, O.P., Kumar, M.S., Baskaran, R., 2014. Identification of novel tyrosine kinase inhibitors for drug-resistant T315I mutant BCR-ABL: a virtual screening and molecular dynamics simulations study. Sci. Rep. 4, 6948. DOI: 10.1038/srep06948

Bhatt, S., Dhiman, S., Kumar, V., Gour, A.,

Manhas, D., Sharma, K., Ojha, P.K., Nandi, U., 2022. Assessment of the CYP1A2 inhibition-mediated drug interaction potential for pinocembrin using *in silico*, *in vitro*, and *in vivo* approaches. ACS omega 7, 20321–20331. https://doi.org/10.1021/acsomega.2c02315

Breijyeh, Z., Karaman, R., 2020. Comprehensive review on Alzheimer's disease: causes and treatment. Molecules 25, 5789. https://www.mdpi.com/1420-3049/25/24/5789#

Cerulli, A., Masullo, M., Montoro, P., Piacente, S., 2022. Licorice (*Glycyrrhiza glabra, G. uralensis, and G. inflata*) and their constituents as active cosmeceutical ingredients. Cosmetics 9, 7. https://www.mdpi.com/2079-9284/9/1/7#

Cichon, N., Grabowska, W., Gorniak, L., Stela, M., Harmata, P., Ceremuga, M., Bijak, M., 2024. Mechanistic and therapeutic insights into flavonoid-based inhibition of acetylcholinesterase: Implications for neurodegenerative diseases. Nutrients 17, 78. https://www.mdpi.com/2072-6643/17/1/78#

da Fonseca, A.M., Caluaco, B.J., Madureira, J.M.C., Cabongo, S.Q., Gaieta, E.M., Djata, F., Colares, R.P., Neto, M.M., Fernandes, C.F.C., Marinho, G.S., 2024. Screening of potential inhibitors targeting the main protease structure of SARS-CoV-2 via molecular docking and approach with molecular dynamics, RMSD, RMSF, H-bond, SASA and MMGBSA. Mol. Biotechnol. 66, 1919–1933. https://doi.org/10.1007/s12033-023-00831-x

El-Nashar, H.A.S., Eldahshan, O.A., El Hassab, M.A., Zengin, G., Elhawary, E.A., 2025. UPLC/MSn analysis of Bougainvillaea glabra leaves and investigation of antioxidant activities and enzyme inhibitory properties. Sci. Rep. 15, 28272. https://doi.org/10.1038/s41598-025-11851-9

Fahim, A.M., 2026. Advances in Computer-Aided Drug Design: From Molecular Docking to AI-Driven Therapeutic Discovery. ASPET Discov. 100024. https://doi.org/10.1016/j.aspetd.2026.100024

Jin, Z., Wei, Z., 2024. Molecular simulation for food protein–ligand interactions: A comprehensive review on principles, current applications, and emerging trends. Compr. Rev. Food Sci. Food Saf. 23, e13280. https://doi.org/10.1111/1541-4337.13280

Kufareva, I., Ilatovskiy, A. V, Abagyan, R., 2012. Pocketome: an encyclopedia of small-molecule binding sites in 4D. Nucleic Acids Res. 40, D535–D540. https://doi.org/10.1093/nar/gkr825

Llorach-Pares, L., Nonell-Canals, A., Avila, C., Sanchez-Martinez, M., 2022. Computer-aided drug design (CADD) to de-orphanize marine molecules: finding potential therapeutic agents for neurodegenerative and cardiovascular diseases. Mar. Drugs 20, 53. https://www.mdpi.com/1660-3397/20/1/53#

Macalino, S.J.Y., Gosu, V., Hong, S., Choi, S., 2015. Role of computer-aided drug design in modern drug discovery. Arch. Pharm. Res. 38, 1686–1701.

DOI 10.1007/s12272-015-0640-5

Mir, S.A., Nayak, B., Khan, A., Khan, M.I., Eldakhakhny, B.M., Arif, D.O., 2024. An exploration of binding of hesperidin, rutin, and thymoquinone to acetylcholinesterase enzyme using multi-level computational approaches. J. Biomol. Struct. Dyn. 42, 11901–11915. https://doi.org/10.1080/07391102.2023.2265492

Nour, H., Hashmi, M.A., Belaidi, S., Errougui, A., El Kouali, M., Talbi, M., Chtita, S., 2023. Design of Acetylcholinesterase Inhibitors as Promising Anti-Alzheimer's Agents Based on QSAR, Molecular Docking, and Molecular Dynamics Studies of Liquiritigenin Derivatives. ChemistrySelect 8, e202301466. https://doi.org/10.1002/slct.202301466

Payen, A., Bateman, J.R., Miller, D., Dhanavanthri Muralidhara, S., Bennett, J.M., 2025. Physiological Changes Linked with Alzheimer's Disease and Related Dementias. Handb. Biol. Pathol. Ment. Disord. 1721–1748. 10. https://doi.org/1007/978-3-031-73368-0_99

Ríos, V., Linares-Pipón, C., Maulén, C., Castro-Álvarez, A., Bradshaw, B., Romero-Parra, J., Cuellar, M.A., Martínez-Cifuentes, M., Parra, C., 2026. Conformationally locked 7-aryl tetrahydroisoquinolines as dual acetylcholinesterase inhibitors and antioxidants: role of intramolecular hydrogen bonding and aryl electronics. Front. Pharmacol. 17, 1797738. https://doi.org/10.3389/fphar.2026.1797738

Shah, M., Patel, K., Kulkarni, U., Yadav, M.R., Patel, A., Nagani, A., 2026. Advances in 1, 3, 4-thiadiazole-based cholinesterase inhibitors: toward novel therapeutics for Alzheimer's disease. Mol. Divers. 1–18. https://doi.org/10.1007/s11030-025-11458-2

Tan, J., Verschueren, K.H.G., Anand, K., Shen, J., Yang, M., Xu, Y., Rao, Z., Bigalke, J., Heisen, B., Mesters, J.R., 2005. pH-dependent conformational flexibility of the SARS-CoV main proteinase (Mpro) dimer: molecular dynamics simulations and multiple X-ray structure analyses. J. Mol. Biol. 354, 25–40. https://doi.org/10.1016/j.jmb.2005.09.012

Xing, S., Li, Q., Xiong, B., Chen, Y., Feng, F., Liu, W., Sun, H., 2021. Structure and therapeutic uses of butyrylcholinesterase: Application in detoxification, Alzheimer's disease, and fat metabolism. Med. Res. Rev. 41, 858–901. https://doi.org/10.1002/med.21745

Yuan, Y., Yu, L., Bi, C., Huang, L., Su, B., Nie, J., Dou, Z., Yang, S., Li, Y., 2025. A new paradigm for drug discovery in the treatment of complex diseases: drug discovery and optimisation. Chin. Med. 20, 40. https://doi.org/10.1186/s13020-025-01075-4